Korean J. Chem. Eng., **24**(5), 881-887 (2007)

Effect of acid concentration and current density on DC etching of aluminum electrolytic capacitor foil

Chiu Yi Hung†, Ou Bin Lung and Lee Yuoh Lien

Department of Mechanical Engineering, National Central University, Chung-Li, Taiwan 320, R.O.C.
(*Received 12 December 2006 • accepted 26 February 2007*)

Abstract−This work studies the effects of acid concentration and current density on etching morphology, microstructure and static capacity of the aluminum foils used in high-voltage electrolytic capacitors. The behavior associated with electrochemical etching was investigated with a potentiostat. The aluminum etching type of DC etching is greatly influenced by the etching potential. The static capacity increased to 0.65 uF/cm^2 with 540 V forming voltage by optimization of the etching parameters used in this work.

Key words: Capacitors, Aluminum Etching, Potential, Current Density

INTRODUCTION

Electronic products are increasingly smaller and thinner. Aluminum electrolytic capacitors are smaller than other electrolytic capacitors but have a great capacity. The procedure for making aluminum electrolytic capacitors includes the manufacture of aluminum foils, etching, forming and assembling. During the procedure, however, etching has the greatest effect on capacity, because many variables are involved in the etching process, leading to, for example, the components and structures of pure aluminum foils, acid concentration, temperature, and current parameters.

Many researchers have studied the effects of the grain size, cubic texture, and elemental impurities on electrochemical DC etching [1-8]. DC etching has been performed to obtain a tunnel-type etching morphology in aluminum foils for high-voltage capacitors [9,10]. Alwitt [11] demonstrated that the tunnel length is dominated by etching temperature. Hebert and Alkire [12] found that a change in the aperture of the tunnels does not affect the growth rate of the tunnels, which is therefore stable. Zhou [13] indicated that the diameter of the tunnel decreased as the amount of sulfuric acid increased. However, few works have focused on the influence of etching potential. Additionally, almost no research has been done on the mechanical analysis of the tension and bending force that anodic etching foil can tolerate. Therefore, this investigation discusses the effect on DC etching by using different concentrations of sulfuric and nitric acid, and of using different current densities to elucidate anodic aluminum etching foil. A potentiostat is adopted to analyze elucidate the relationship between the potential and the type of etching. The results can help to elucidate the mechanical characteristics of the etching foil.

EXPERIMENTAL PROCEDURE

The specimen in this experiment is high purity aluminum foil, with 99.99% purity and 110 μm of thickness. Its main composition is illustrated in Table 1. The specimen was pre-treated with phosphoric acid in order to form a smooth oxidation film on the surface. Electric current came directly from a power supplier. The current density variation in this experiment was 0.02-0.2 A/cm^2. Two graphite electrode plates of 155×65×8 mm^3 size were used for electro etching, with a gap of 25 mm between them. The specimen was placed parallel to the two electrode plates with a distance of 10 mm between each of them. The electro etching bath was a 5-litre glass beaker filled with conducting solution. The variation of sulphuric acid concentration was 1-9 N; and nitric acid, 0.05 N-0.90 N. Temperature of the solution was measured by alcohol thermometer, controlled by heating blender and temperature controller, and set to 32± 2 °C. Using a potentiostat (AUTOLAB/PGSTAT30), the required current density and testing condition were inputted by using the method of chronopotentiometry to a computer, which then recorded the variation between voltage and time under different electro etching conditions. Ag/AgCl electrode was used as reference electrode, and high purity platinum filament was used as counter electrode.

Table 1. Main composition of the specimens (ppm)

Fe	Si	Cu	Mn
24	31	18	1

The forming process in this experiment followed the EIAJ (Electronic Industries Association of Japan) code; the forming process made by EIAJ is the most popular process in the electrolytic industry. 540 Vfe forming solution of the EIAJ code category 4 was used. The solution was made by adding 100 g of boric acid to 1,000 ml of pure water. The static capacity measuring solution was the EIAJ assigned measuring solution for high voltage anode aluminum foil formation. It was made by adding 90 g of amine pent borate to 1,000 ml of pure water. The oxide replica of the etching views was done by applying a small amount of epoxy resin to the surface of the forming foil, and immersing the foil into bromine methanol solution (10% Br_2/CH_3OH). The cross section of the electro etching aluminum foil was then examined by OLYMPUS's BX60M optical microscope (OM). The size and distribution of etched holes on the electro etching foil's surface and the oxide replica specimen were examined by scanning electron microscope (SEM, HITACHI S-

†To whom correspondence should be addressed.
E-mail: s9323051@cc.ncu.edu.tw

2150). Flow chart of the experiment is illustrated in Fig. 1.

RESULTS AND DISCUSSION

1. Effect on Sulfuric Acid Concentration

Reactions (1) and (2) are the reactions of aluminum dissolution.

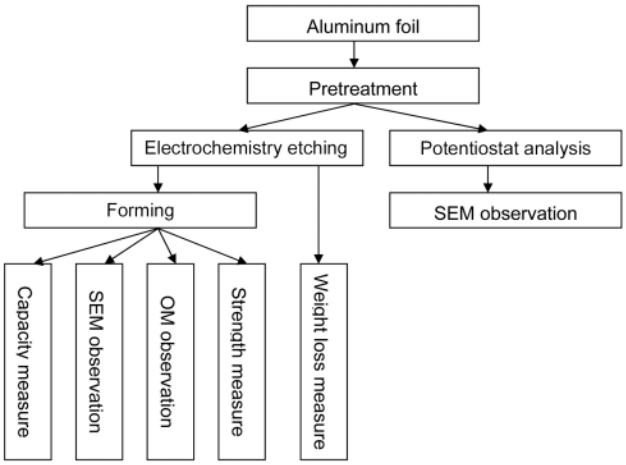

Fig. 1. Flow chart of the experimental procedure.

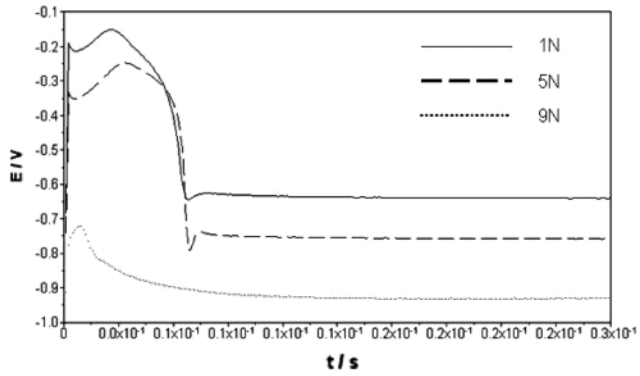

Fig. 2. The relationship between potential and time under different sulfuric acid concentrations.

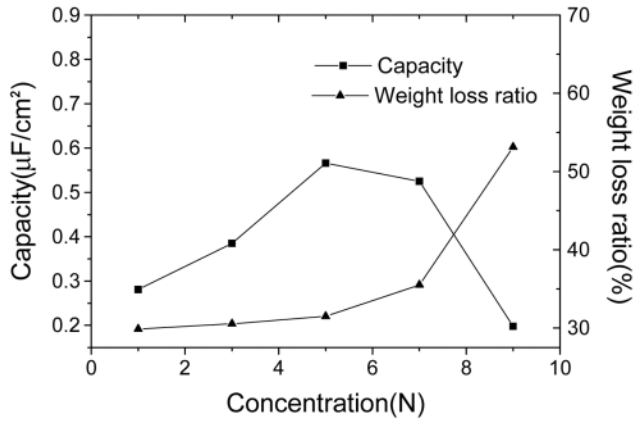

Fig. 3. Correlation curve between static capacity and weight loss ratio under different sulfuric acid concentrations.

$$2Al+6HCl \rightarrow 2AlCl_3+3H_2 \quad (1)$$

$$2Al+3H_2SO_4 \rightarrow Al_2(SO_4)_3+3H_2 \quad (2)$$

Tunnel growth occurs only in the <110> crystallographic directions. The dissolving tip face is a flat and smooth (100) plane. The aluminum foil surface and the tunnel sidewalls can be attributed to the presence of a surface oxide film which could protect aluminum from Cl^- and SO_4^{2-} attack. As the tunnel tip dissolves, new oxide film continuously forms on the sidewalls. Sidewall passivation and tunnel tip dissolution is the mechanism of tunnel growth. Fig. 2 plots the relationship between potential and time at various sulfuric acid concentrations. It captures the electrochemical behavior associated with electro etching by using a potentiostat. During electro etching, electrical potential will initially rise to a maximum, from which it

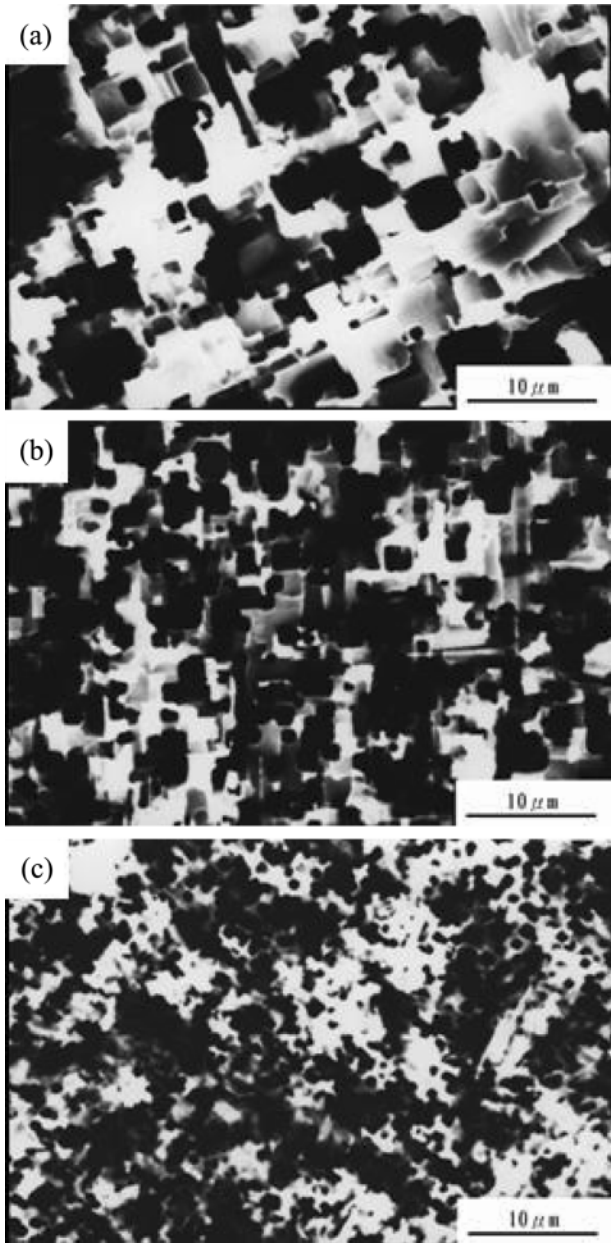

Fig. 4. SEM photographs for specimen from different sulfuric acid concentrations: (a) 1 N, (b) 5 N, (c) 9 N.

falls to a constant value. The highest potential is Eb (breakdown potential); the constant potential is Ep (pitting potential of solution). If Eb is low, then the weak points of the oxidized cover will be easily broken by corrosive ions, beginning pit etching. Eb decreases as the concentration of sulfuric acid increases. The data reveal that the numbers of etched pit increased with the concentration of sulfuric acid. Ep plays an important role during tunnel etching. On the surface and sidewalls it needs an oxide film to protect aluminum. Local Eps (etching potential of sidewall and surface) would be maintained in the passive potential zone. Tunnel tip dissolution, needs the local Ept (etching potential of tunnel tip) in the depassivative potential zone. There is a critical Ep that makes Eps in the passive potential zone and Ept in the depassivative potential zone. Fig. 1 shows Ep decreases as the concentration of sulfuric acid increases.

Fig. 3 plots the static capacity and weight loss ratio after the testing pieces were etched at various concentrations of sulfuric acid. The weight loss increases with the concentration of sulfuric acid. 9 N has a weight loss ratio of 53.1%, indicating serious spallation during etching, which is responsible for poor static capacity. Note that with the standpoint of the potential, Ep declined as the concentration of sulfuric acid increased. From 1 N-5 N, the numbers of tunnels increased as the potential decreased, causing the proper surface expansion to form at 5 N. When the concentration of sulfuric acid was over 5 N, the drop in the potential changed tunnel etching to surface etching and decreased the static capacity.

Fig. 4 presents the SEM results of the tested pieces after etching. The figure shows that square pits appeared in all tested pieces, and the diameter of the pits obviously decreased as the concentration of sulfuric acid increased. That is, specimens with a high sulfuric con-

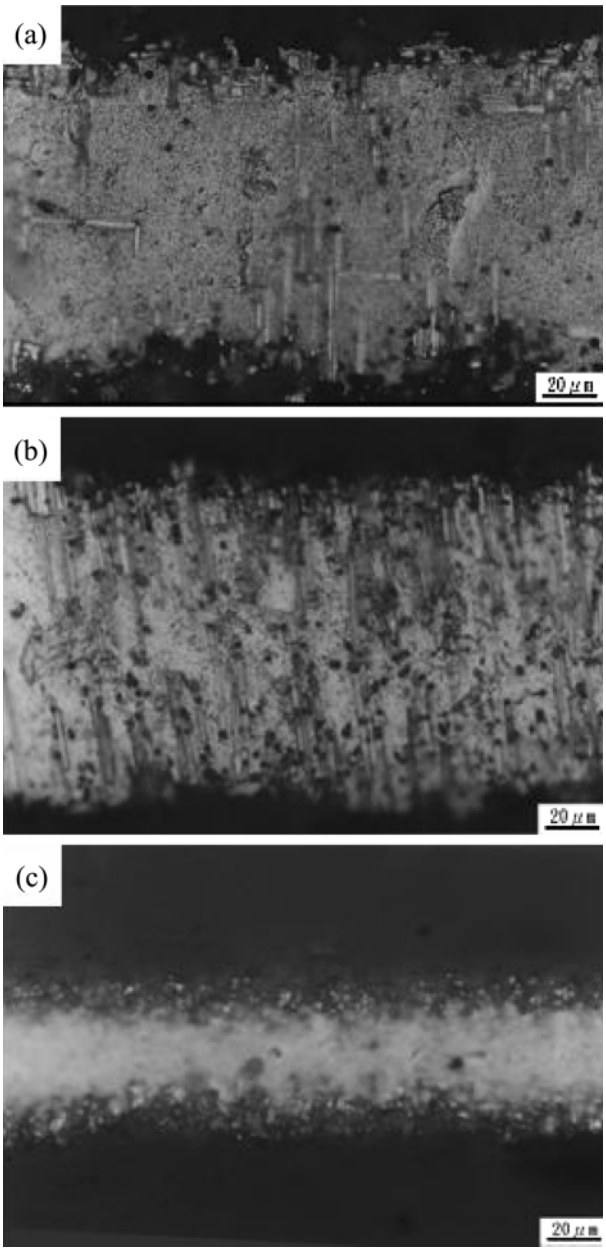

Fig. 5. Cross-section of etched morphology for specimen from different sulfuric acid concentrations: (a) 1 N, (b) 5 N, (c) 9 N.

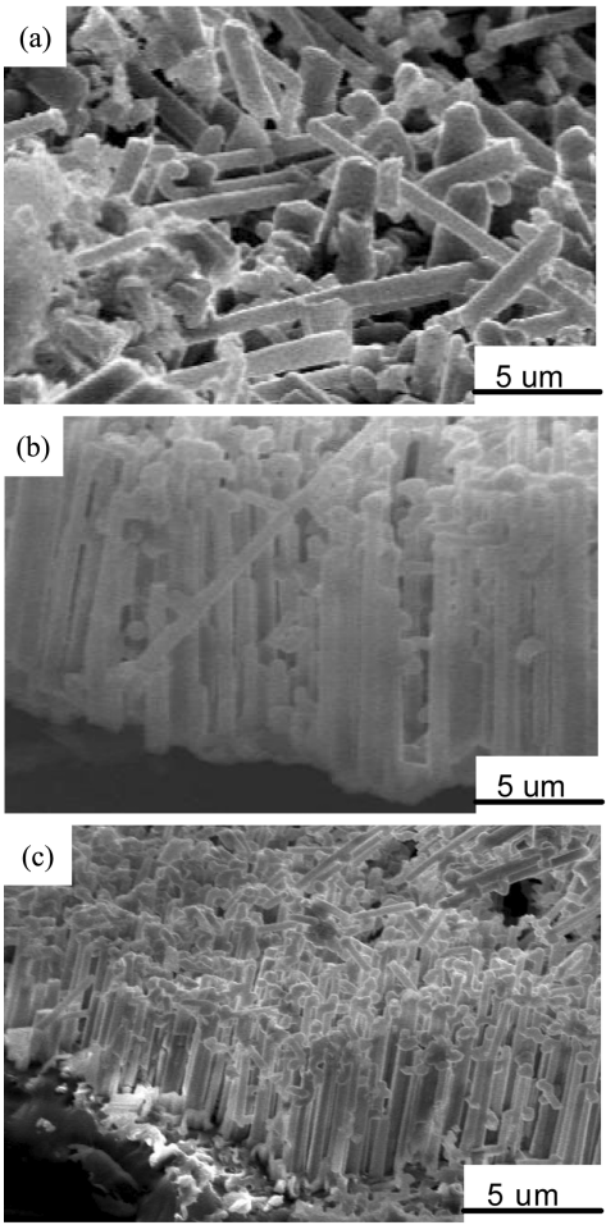

Fig. 6. SEM views of oxide replica from different sulfuric acid concentrations: (a) 1 N, (b) 5 N, (c) 9 N.

centration had a higher wall passive speed which formed smaller etched pits. Fig. 5 displays images of the specimen obtained by OM. A few tunnels were formed in 1 N, while 9 N supported strong surface etching, which sheared the aluminum foil from 100 um to 65 um. Fig. 6 presents the SEM views of the oxide replica in various concentrations of sulfuric acid. The 5 N acid exhibits a greater expansion of surface area. This result is consistent with the OM image in Fig. 5. Fig. 6 reveals that the tunnel lengths in 1 N and 5 N acids are almost the same; 9 N yields a shorter tunnel because of surface etching, but its actual growing length is close to that in 1 N and 5 N, supporting Herbert and Alkire's [12] view that the size of the tunnel does not influence its growth rate.

Fig. 7 shows tensile strength and bending strength in various concentrations of sulfuric acid. Figs. 3 and 7 reveal that as the weight loss ratio increases, the tensile strength declines, because a lower force can break the specimen with a high weight loss ratio. Theoretically, the bending strength follows the same trend as the tensile strength and the weight loss ratio. However, the bending strength was lowest in 5 N acid. Comparing Fig. 5 with 7 indicates that the bending strength is correlated with the length of the non-etched area in the center of the aluminum foil. Less etching of the center of the aluminum foil corresponds to higher bending strength.

The aforementioned results reveal that there is a proper etching potential for forming a large number of tunnels. If Ep is high (1 N, 3 N), Ept is near the passive potential zone. Only few surface pits can keep growing into tunnels. On the other hand, the tunnel etching type turns to surface etching type while the Ep is low, which makes Eps and Ept all be in the depassivative potential zone.

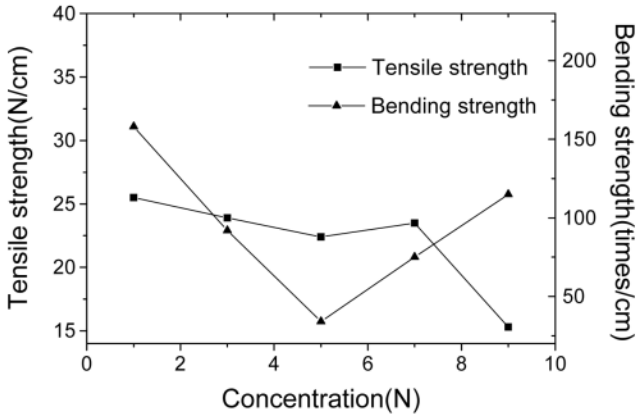

Fig. 7. The relational chart of tensile and bending strength from different sulphuric acid concentrations.

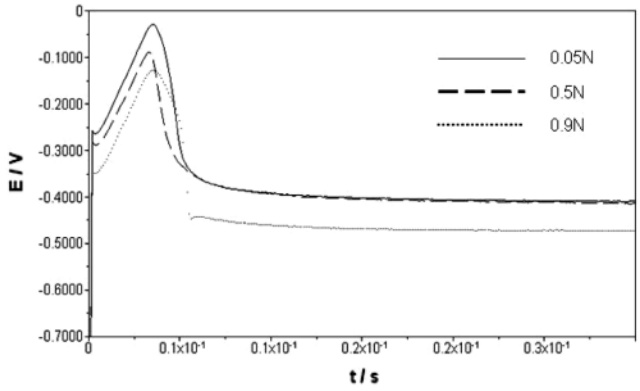

Fig. 8. The relationship between potential and time under different nitric acid concentrations.

2. Effect of Nitric Acid Concentration

The sulphuric acid concentration is 5 N and the hydrochloric acid is 0.9 N in this part of the experiment. The variation of nitric acid concentration is 0.05-0.9 N. Fig. 8 plots the relationship between potential and time at different nitric acid concentrations. The Eb and Ep of these conditions substantially exceed those in Fig. 2.The reaction between nitric acid and aluminum is shown as reaction (3). Al_2O_3 is an oxide film which could cover aluminum and make passivation of aluminum. Addition of nitric acid would inhibit the depassivation of tunnel tip during tunnel growth and have serious influence on etching morphology of aluminum foil. Figs. 2 and 8 show that Ep raises 380 mV when addition of nitric acid is about 0.05 N. And Ep moves from critical potential zone to passive potential zone.

$$2Al+6HNO_3 \rightarrow Al_2O_3+3H_2O+6NO \quad (3)$$

Fig. 9 displays the effects of the nitric acid concentration on the static capacity and weight loss ratio after electrochemical etching. The weight loss ratio is fairly low, and the static capacity is around 0.2 μF/cm^2. Fig. 10 presents the tensile strength and bending strength

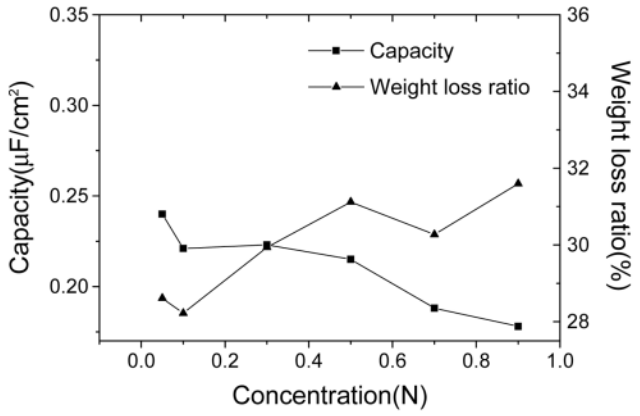

Fig. 9. Correlation curve between static capacity and weight loss ratio under different nitric acid concentrations.

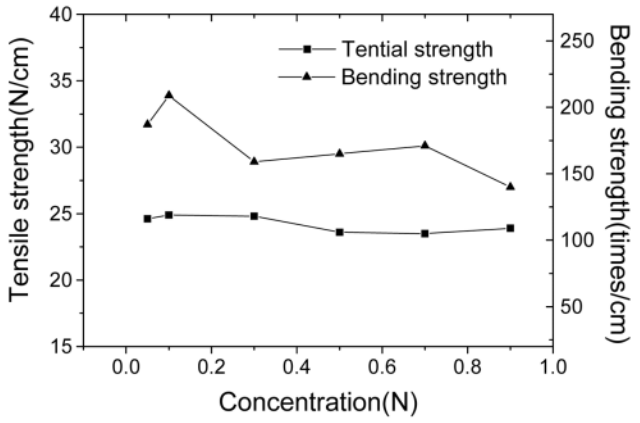

Fig. 10. The relational chart of tensile and bending strength from different nitric acid concentrations.

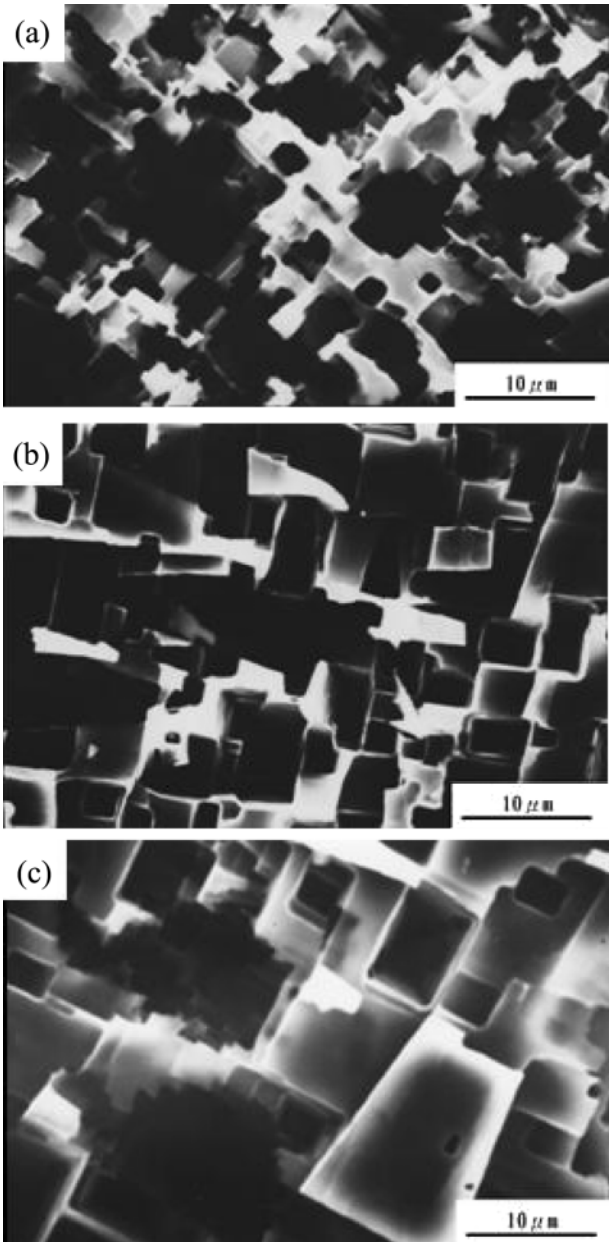

Fig. 11. SEM photographs for specimen from different nitric acid concentrations: (a) 0.05 N, (b) 0.5 N, (c) 0.9 N.

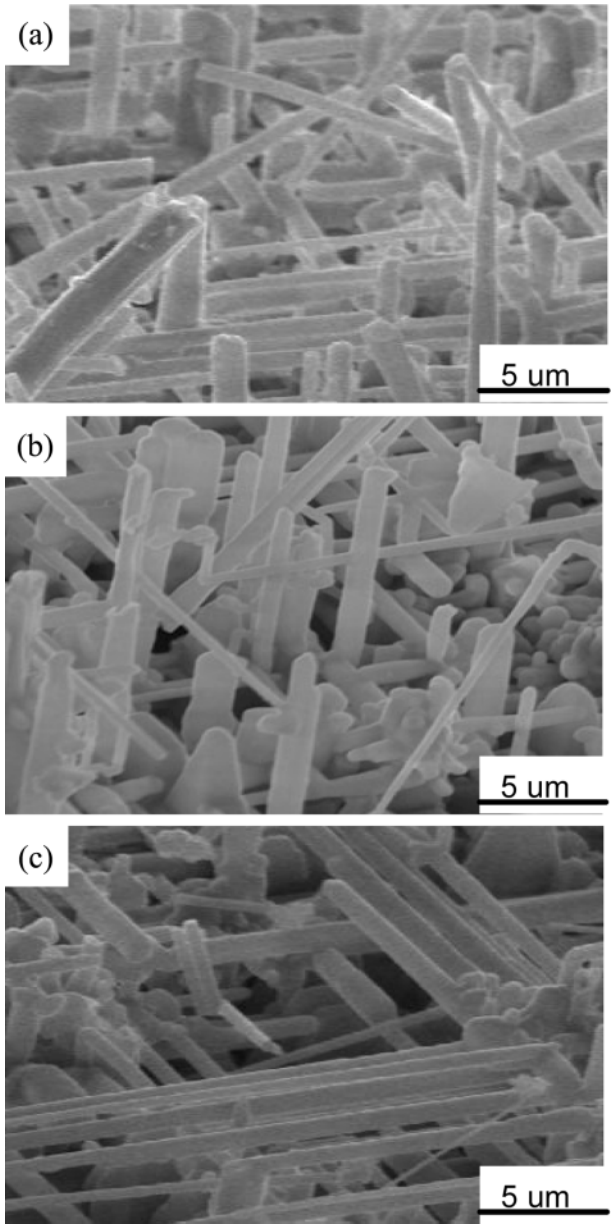

Fig. 12. SEM views of oxide replica from different nitric acid concentrations: (a) 0.05 N, (b) 0.5 N, (c) 0.9 N.

in various concentrations of nitric acid. Since these conditions do not support the formation of a large number of vertical tunnels and have produced a low weight loss ratio, the bending and tensile strength are high. Fig. 11 shows the SEM images of the specimen at various nitric acid concentrations. A higher concentration corresponds to larger etched pits on the surface. The surface pits in Fig. 11 are larger than those in Fig. 4 because Eb was high. Therefore, the numbers of the start points of the corrosion were less than those in Fig. 4 and result in the formation of large etching pits. Fig. 12 presents the SEM views of the oxide replica at various nitric acid concentrations, and elucidates why the static capacity is low under these conditions, mainly because the etching potential considerably exceeds the proper potential at which large numbers of vertical tunnels can be formed. Most pits under these conditions could not continue to grow because of the addition of nitric acid. Perhaps, adding nitric acid passivates aluminum during electrochemical etching, and so cannot be added for tunnel etching.

3. Effect on Current Density

The current densities in this experiment were 0.02 A/cm^2, 0.05 A/cm^2, 0.1 A/cm^2 and 0.2 A/cm^2. The sulphuric acid concentration is 5 N, the hydrochloric acid is 0.9 N and without addition any nitric acid in this part of experiment. The period of electro etching will be tuned to fix the total electric current. Fig. 13 plots the relationship between potential and time at various current densities. Although the range of current densities is large, the etching potentials are quite close to each other. It means that in this part of experiment, the Ep of each current density is close to the critical potential which is suitable for tunnel to grow. Fig. 14 plots the effects of cur-

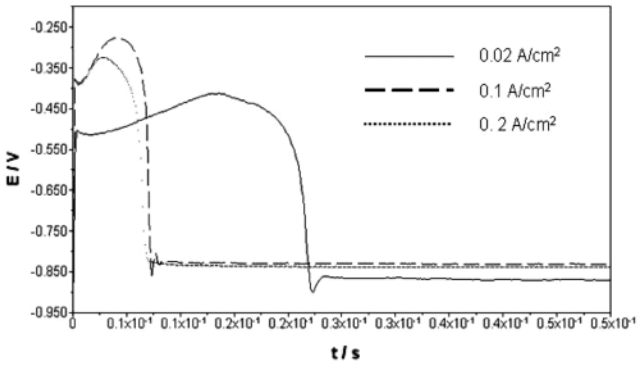

Fig. 13. The relationship between potential and time under different current densities.

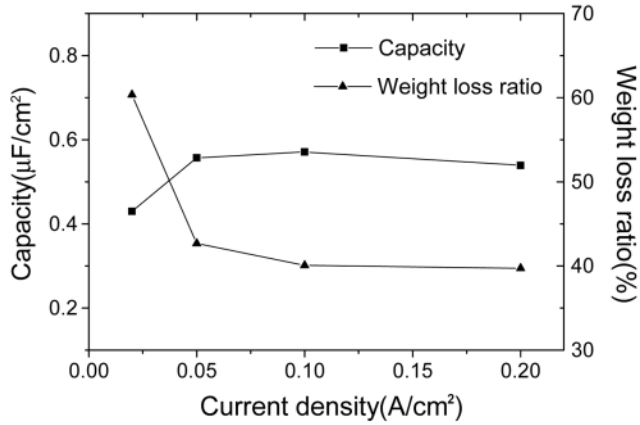

Fig. 14. Correlation curve between static capacity and weight loss ratio under different current densities.

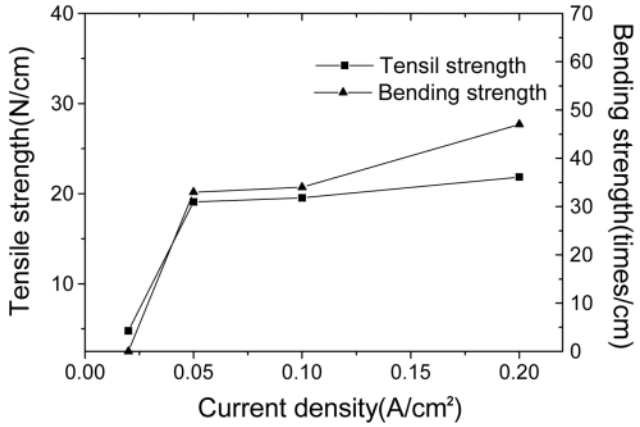

Fig. 15. The relational chart of tensile and bending strength from different current densities.

rent density on the static capacity and weight loss ratio after electrochemical etching: the weight loss ratio decreased as the current density increased, for all other conditions fixed.

According to Faraday's Law, when the total coulomb of each current density is the same, the quantity of aluminum corrosion should also be the same. It is not reasonable that weight loss ratio decreased as the current density increased. The possible reason could be that not only reactions (1) and (2) occur at the anode but also reaction (4), and these three reactions will compete to cost current with others. Reactions (1) and (2) will have higher ratio in low current density than in high current density; it means that in low current density reactions (1) and (2) will have better current efficiency and higher weight loss ratio.

$$2H_2O \rightarrow 4H^+ + O_2 + 4e^- \quad (4)$$

Fig. 15 plots tensile and bending strength at various current densities. The tensile strength increased with the current density, mainly because, as mentioned above, a higher current density corresponds to a lower weight loss ratio, and greater tensile strength. Fig. 16 presents OM images obtained at various current densities. Fig. 16(a)

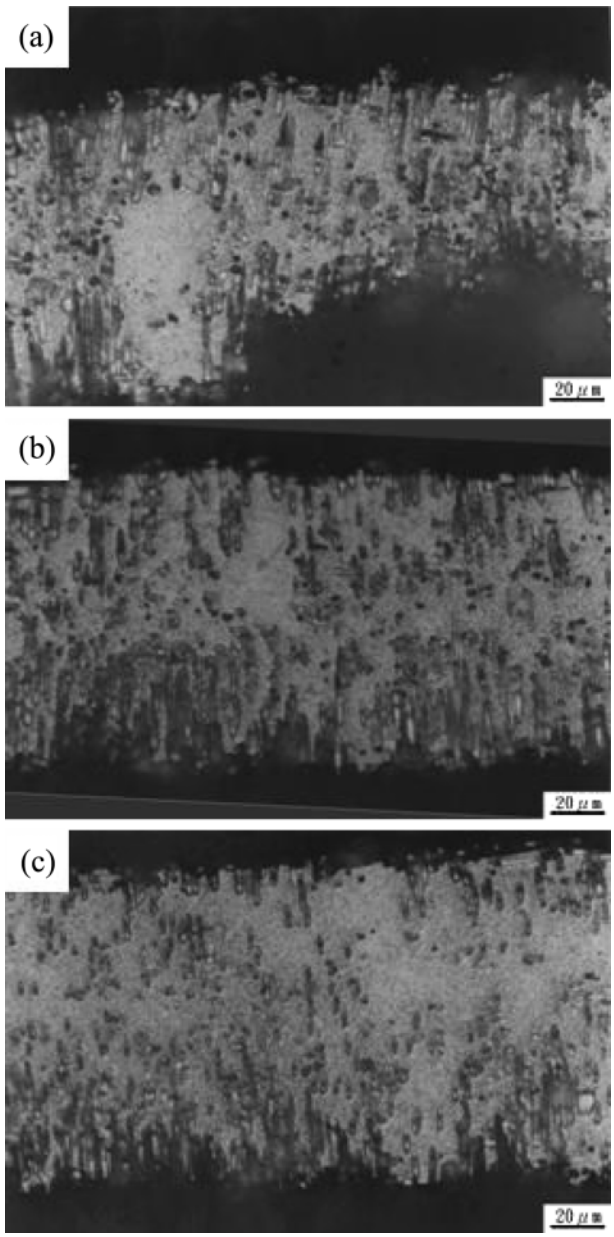

Fig. 16. Cross-section of etched morphology for specimen from different current densities: (a) 0.02 A/cm², (b) 0.1 A/cm², (c) 0.2 A/cm².

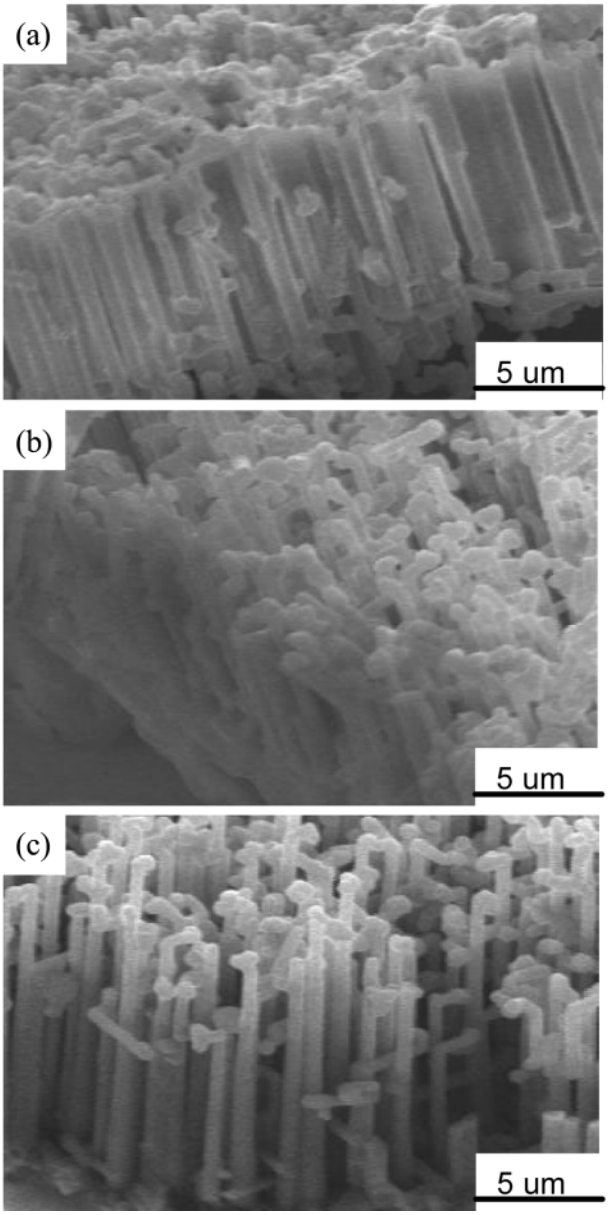

Fig. 17. SEM views of oxide replica from different current densities: (a) 0.02 A/cm^2, (b) 0.1 A/cm^2, (c) 0.2 A/cm^2.

shows serious local corrosion, which may explain why the bending strength of 0.02 A/cm^2 is zero, and the sample cannot tolerate any bending force. Fig. 17 presents the SEM images of the oxide replicas at various current densities. The size and numbers of these samples are very similar. These results indicate that Eb and Ep are very close, even over a large range of current densities. Each is responsible for a tunnel etching morphology and, consequently, high static capacity.

CONCLUSION

The experimental results above support the following conclusions.

This work reveals that an optimum pitting potential is required to extend pit etching vertically to form tunnels without surface etching. If the pitting potential is excessive, it cannot form many vertical etched tunnels; if it is too low, then the type of etching is changed from pitting to uniform etching. Besides Zhou [13], who indicated that the diameter of the tunnel decreased as the amount of sulfuric acid increased, this study also finds that as the etching potential decreases, the pits on the etched surface become smaller.

Since nitric acid causes passivation, adding nitric acid to the specimen increases the etching potential above the optimal pitting potential. Therefore, despite the formation of large pits on the surface of the aluminum foil, most cannot continue to be vertically etched to form etched tunnels. Therefore, nitric acid does not help to increase the expansion of the etched surface.

Despite substantial electric current density variation, the pitting potential varies little with the conditions and large numbers of etched tunnels are formed. The static capacity is therefore relatively high. Specimens with higher current density have a lower electric current efficiency, and therefore, a lower weight loss rate.

ACKNOWLEDGMENT

The authors would like to express their appreciation for the financial support of the National Science Council of the Republic of China under grant No. NSC92-2622-E008-025-cc3.

REFERENCES

1. K. Arai and T. Suzuki, *Light Mata.*, **31**, 675 (1981).
2. R. Bakish, E. Z. Border and R. J. Kornhass, *J. Electrochem. Soc.*, **109**, 791 (1962).
3. R. Bakish, *Electrochem. Technol.*, **6**, 192 (1968).
4. Z. Q. Zheng and W. B. Zhang, *J. China Inst. South Inst. Mining Central Metal.*, **1**, 111 (1983).
5. T. Suzuki, K. Arai, M. Shiga and Y. Nakamura, *Metall. Trans.*, **16A**, 27 (1985).
6. H. C. Chen and B. L. Ou, *Journal of Materials Science: Materials in Electronics.*, **15**, 819 (2004).
7. J. H. Choi and S. B. Kim, *The Korean Journal of Chemical Engineering*, **11**, 178 (1994).
8. S. J. Kim and J. Y. Ko, *The Korean Journal of Chemical Engineering*, **23**, 847 (2006).
9. Z. Hen and Z. Weibin, *Mater. Sci. Engi.*, **B3**, 479 (1989).
10. N. Osawa and K. Fukuoka, *Corros. Sci.*, **42**, 585 (2000).
11. W. Lin, G. C. Tu, C. F. Lin and Y. M. Peng, *Corrosion Science*, **38**, 889 (1996).
12. K. Hebert and R. Alkire, *J. Eletrochem. Soc.*, **135**, 2447 (1988).
13. Y. Zhou and K. R. Hebert, *J. Eletrochem. Soc.*, **145**, 2100 (1998).